

Supporting information for the paper

Blue Emitting Undecaplatinum Cluster

Indranath Chakraborty, Radha Gobinda Bhui, Shridevi Bhat and T. Pradeep*
*DST Unit of Nanoscience (DST UNS), Department of Chemistry, Indian Institute of
Technology Madras, Chennai 600036, India.*

S. No.	Description	Page No.
1	Experimental section and instrumentation	2
2	Chromatogram and UV/Vis of crude Pt cluster	4
3	MALDI MS and UV/Vis spectra of isolated 2 and 3	5
4	SEM/EDAX of isolated 2 and 3	6
5	Laser intensity dependent MALDI MS and comparison with $\text{Ag}_{44}(4\text{-FTP})_{30}$ cluster	7
6	DLS of Pt_{11} cluster	8
7	Full range ESI MS	9
8	ESI MS under different ionizing conditions	10
9	DLS of Pt_{11} cluster	11
10	SEM/EDAX of Pt_{11} cluster	12
11	FT IR spectra of the thiol and Pt_{11} cluster	13
12	XPS survey spectrum	14
13	Expanded XPS of C 1s and S 2p regions	15
14	PXRD of Pt_{11} cluster	16
15	^{195}Pt NMR of K_2PtCl_6 standard	17
16	Time dependent UV/Vis and solvent compatibility	18

Supporting Information 1

Materials and methods:

1. Chemicals

Chloroplatinic acid (H_2PtCl_6 , 99% Aldrich), sodium borohydride (NaBH_4 , 99.9%, Aldrich); 4-(tert-butyl) benzyl mercaptan (BBSH, 98%, Aldrich); ethanol (Changshu Yangyuan Chemical, China, AR grade) and toluene (Ranken) were used in this synthesis. All the chemicals were commercially available and were used without further purification.

2. Synthesis of $\text{Pt}_{11}(\text{BBS})_8$

The synthesis of Pt cluster protected by BBSH (4-(tert-butyl) benzyl mercaptan) involves the following steps. Initially, 20 mg of $\text{H}_2\text{PtCl}_6 \cdot 6\text{H}_2\text{O}$ and 60 μL of 4-(tert-butyl) benzyl mercaptan (BBSH) were ground and mixed well at room temperature in a clean mortar using a pestle. The color changes to orange yellow showing the formation of platinum thiolate. To this mixture, 40 mg of solid NaBH_4 was added and the contents were ground well. The orange yellow color changes to deep brown suggesting the reduction of Pt and formation of Pt clusters. Then 5 mL of ethanol was added to remove the extra thiol and it was centrifuged for 4 minutes at 4000 rpm. Centrifugate was discarded and the precipitate was re-extracted with 7 mL of toluene to get the crude cluster which is deep yellow in color.

3. Instrumentation:

UV-Vis spectra were measured with a Perkin Elmer Lambda 25 spectrometer in the range of 200-1100 nm. Luminescence measurements were carried out on a Jobin Vyon NanoLog instrument. The band passes for excitation and emission were set as 2 nm. HPLC measurement was done using a Shimadzu HPLC system equipped with a normal phase column (Shimadzu) and a UV/Vis detector. Matrix-assisted desorption ionization mass spectrometry (MALDI MS)

studies were conducted using a Voyager-DE PRO Biospectrometry Workstation from Applied Biosystems. DCTB (trans-2-[3-(4-tert-Butylphenyl)-2-methyl-2-propenylidene]malononitrile) was used as matrix (at 1:100 ratio of sample to matrix). A pulsed nitrogen laser of 337 nm was used for the MALDI MS studies. Mass spectra were collected in positive ion mode and were averaged for 200 shots. ESI MS measurements were done on one LTQ XL mass spectrometer from Thermo Scientific, San Jose, CA. Methanol-toluene mixture was used for this experiment. CsOAc was used as the external ionizing agent. The spectra were collected in positive mode. High resolution transmission electron microscopy of clusters was carried out with a JEOL 3010 instrument. The samples were drop casted on carbon-coated copper grids and allowed to dry under ambient conditions. Scanning electron microscopic (SEM) and energy dispersive X-ray (EDAX) analyses were performed with a FEI QUANTA-200 SEM. For measurements, samples were drop casted on an indium tin oxide (ITO) coated glass and dried in vacuum. FT-IR spectra were measured with a Perkin Elmer Spectrum One instrument. X-ray photoelectron spectroscopy (XPS) measurements were conducted using an Omicron ESCA Probe spectrometer with polychromatic MgK α X-rays ($h\nu=1253.6$ eV). The samples were spotted as drop-cast films on a sample stub. Constant analyzer energy of 20 eV was used for the measurements. DLS was done with a Horiba instrument. Powder XRD patterns of the samples were recorded using PANalytical X'pertPro diffractometer. A thin film of cluster was made on a glass slide which was used for this experiment. ^{195}Pt NMR measurements were performed using a Bruker (700 MHz) instrument. K_2PtCl_6 was taken as standard. Whole Pt chemical shift (-3000 to +11800 ppm) range was covered for the Pt_{11} cluster to see the peaks. Overnight runs were necessary to observe adequate signals.

4. QY calculation

It has been calculated by taking R_6G as a reference¹ using the following equation

$$\Phi = \Phi_r \frac{A_r}{I_r} \frac{I}{A}$$

where Φ is the quantum yield, I is the measured integrated emission intensity, A is the absorbance and the subscript “r” refers to the reference.

Supporting Information 2

Chromatogram and UV/Vis of the crude Pt cluster

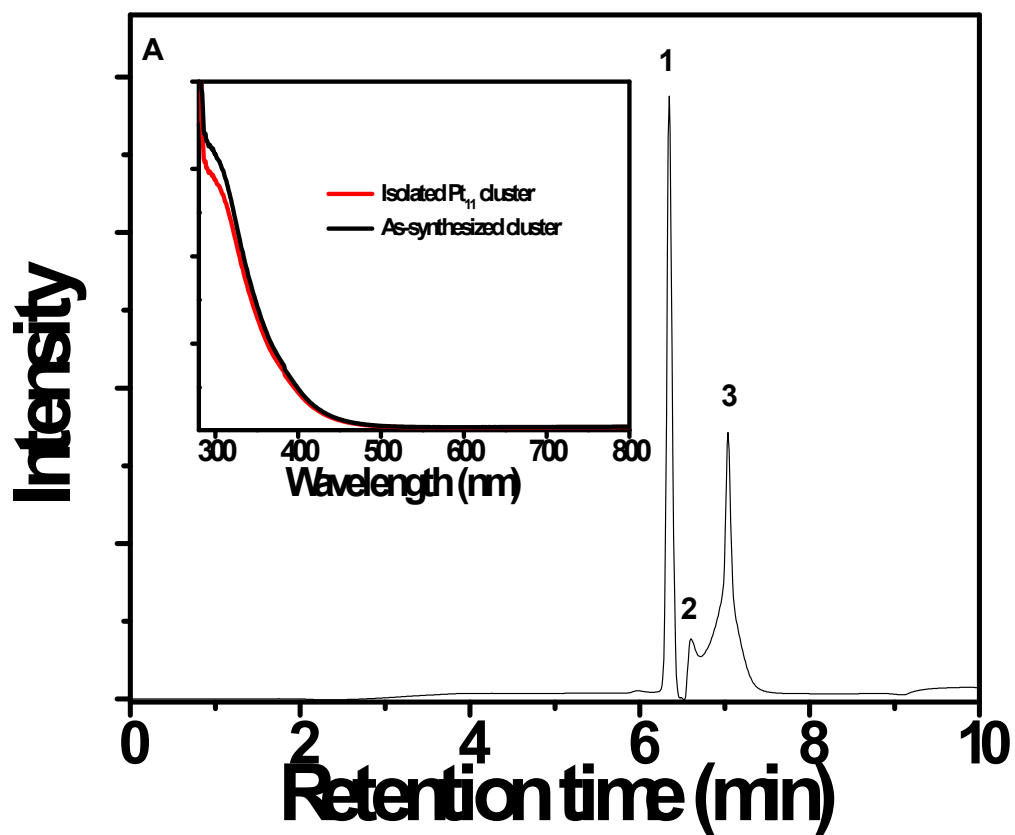


Fig. S2. Chromatogram of as-synthesized Pt cluster taken with a normal phase column with UV/Vis detector. Well separated cluster (peak 1) was isolated at 6.3 min retention time along with two other features (marked 2 and 3). Isolated (1) shows the same UV/Vis as the as-synthesized cluster (data shown in the inset). Other peaks do not show any characteristic UV/vis features.

Supporting Information 3

MALDI MS and UV/Vis spectra of isolated 2 and 3

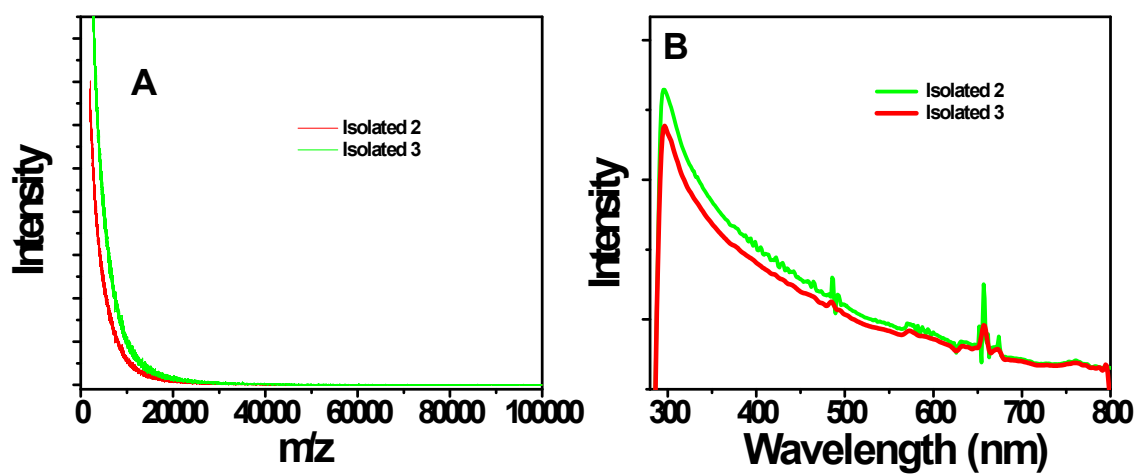


Fig. S3. MALDI MS (A) and UV/Vis (B) spectra of isolated 2 and 3, respectively. The data suggest that there are decomposed products.

Supporting Information 4

SEM/EDAX of isolated 2 and 3

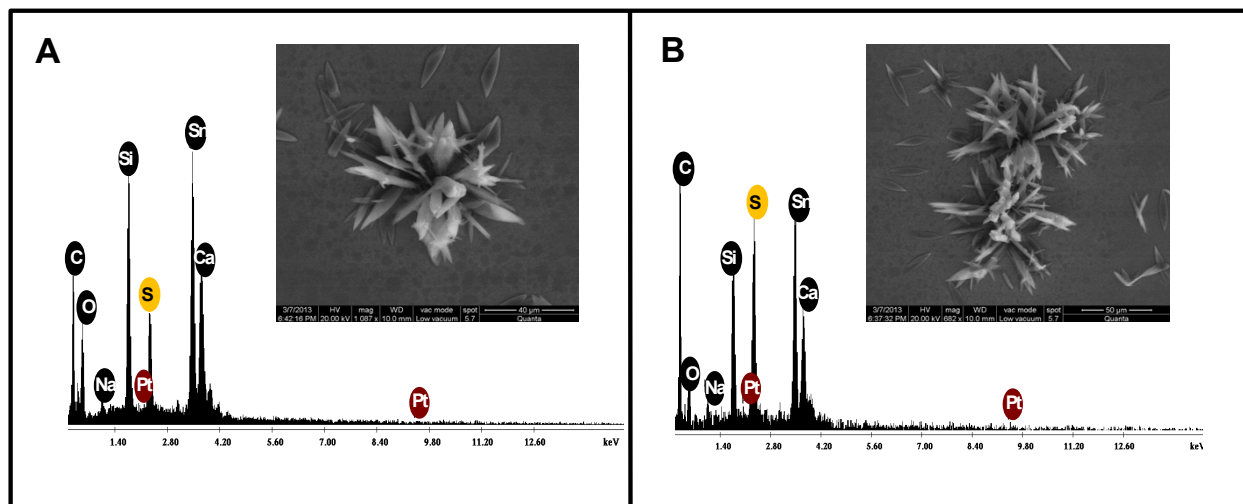


Fig. S4. SEM/EDAX of the isolated 2 (A) and 3 (B), spotted on an ITO plate. Ca, Sn, Si are from the plate. Inset show the corresponding SEM images.

Supporting Information 5

Laser intensity-dependent MALDI MS and comparison with $\text{Ag}_{44}(\text{4-FTP})_{30}$ cluster

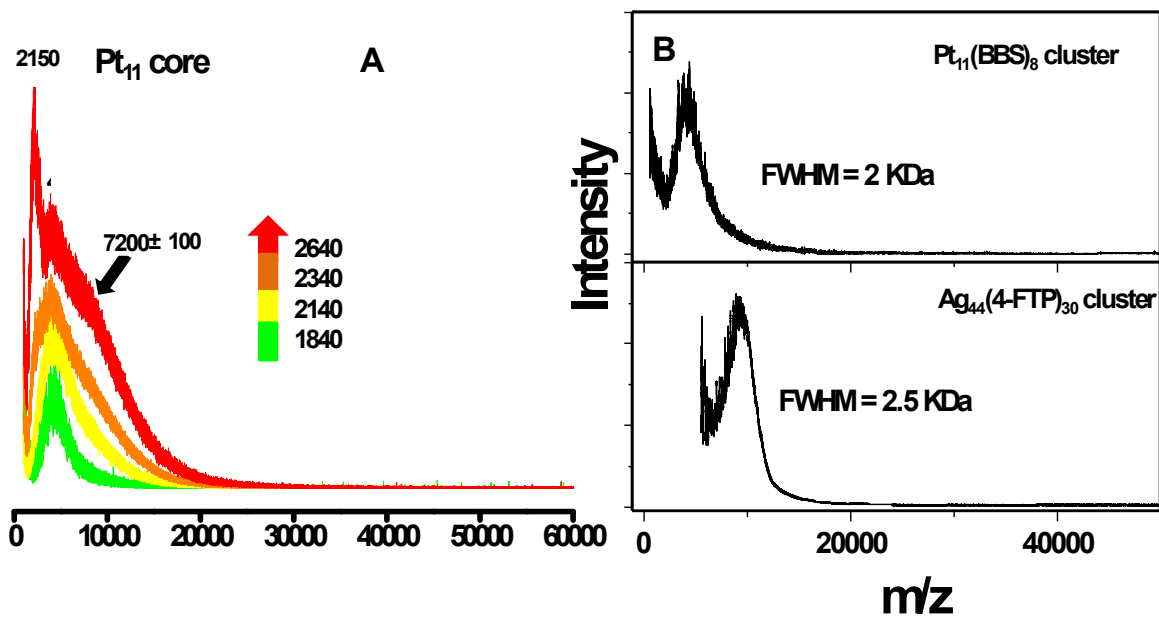


Fig. S5. A: Laser power dependency on the $\text{Pt}_{11}(\text{BBS})_8$ cluster. The numbers on the right of the figure are laser intensities shown by the instrument. **B:** Comparative MALDI mass spectra of $\text{Pt}_{11}(\text{BBS})_8$ and $\text{Ag}_{44}(\text{4-FTP})_{30}$ cluster.

Supporting Information 6

Full range ESI MS

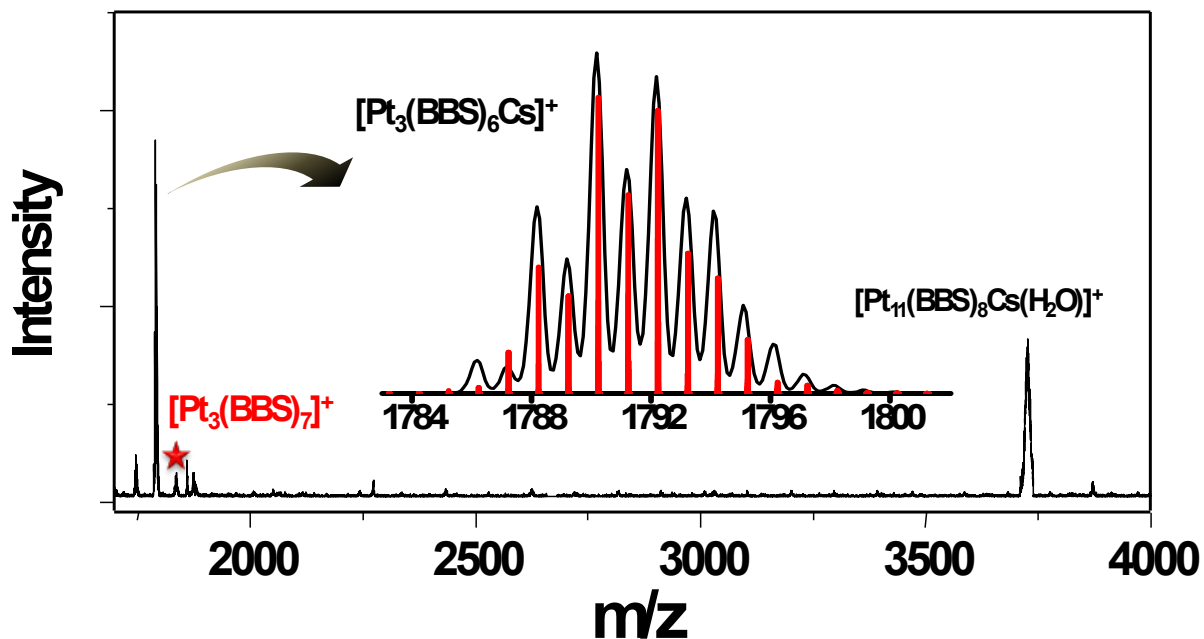


Fig. S6. Full range ESI mass spectrum of the purified cluster. Inset shows the expanded view of a fragment. The mass spectrum (black) shows nearly an exact match with the calculated spectrum (sticks).

Supporting Information 7

ESI MS of $\text{Pt}_{11}(\text{BBS})_8$ cluster under different ionizing conditions

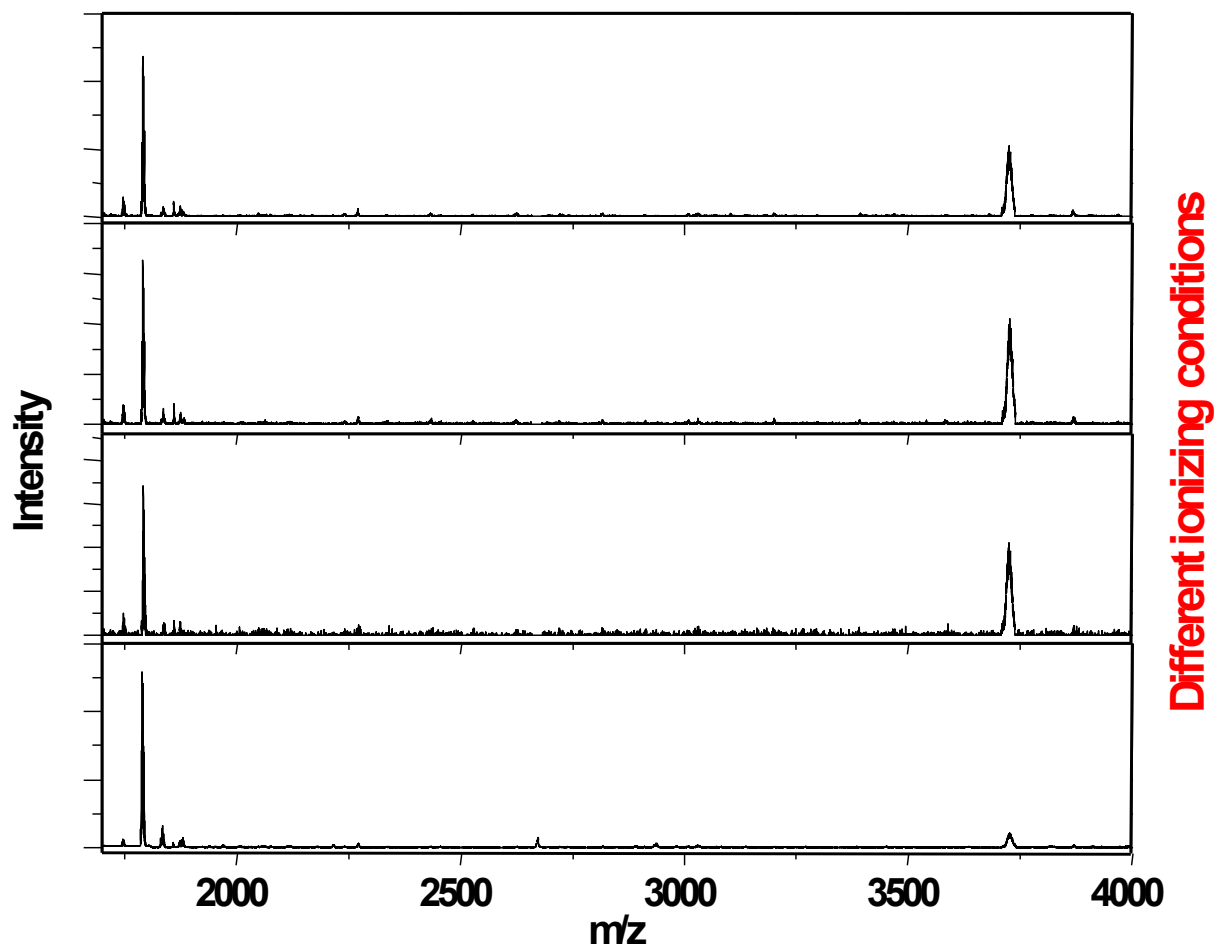


Fig. S7. ESI MS spectra of $\text{Pt}_{11}(\text{BBS})_8$ cluster under different ionizing conditions. In this case, the instrument parameters have been varied to get a maximum intense molecular peak.

Supporting Information 8

TEM image and size distribution of the $\text{Pt}_{11}(\text{BBS})_8$ cluster

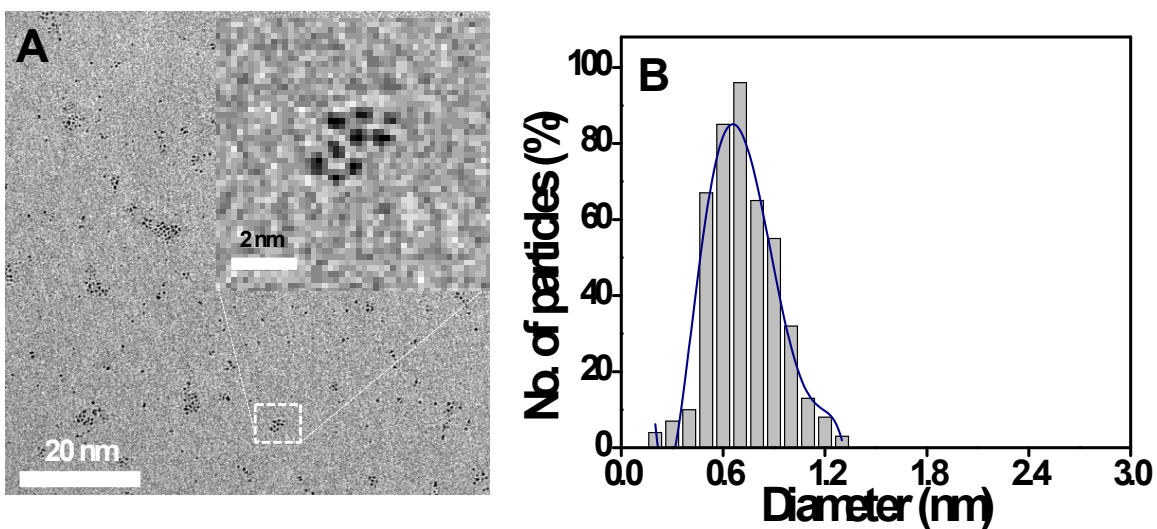


Fig. S7. A: HRTEM image of the Pt_{11} cluster shows tiny particles. Inset shows an expanded view of the selected area. B: Size distribution fitted with an appropriate polynomial. The average diameter was found to be 0.66 nm. Electron beam-induced damage causes an increased particle size distribution.

Supporting Information 9

DLS of the $\text{Pt}_{11}(\text{BBS})_8$ cluster

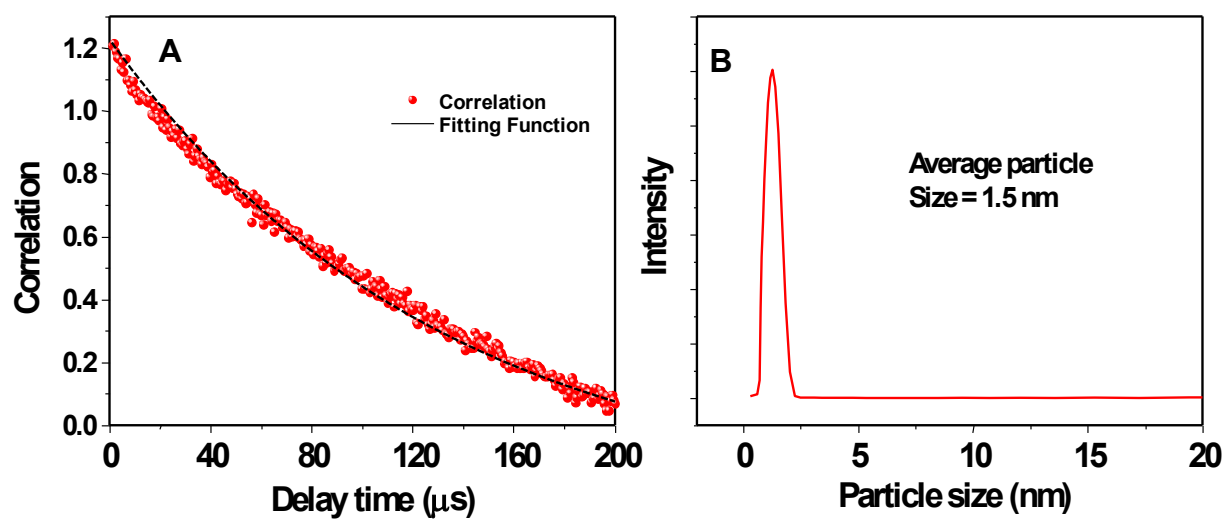


Fig. S9. DLS correlation (A) and size distribution curve (B) of the cluster.

Supporting Information 10

SEM/EDAX of the Pt₁₁(BBS)₈ cluster

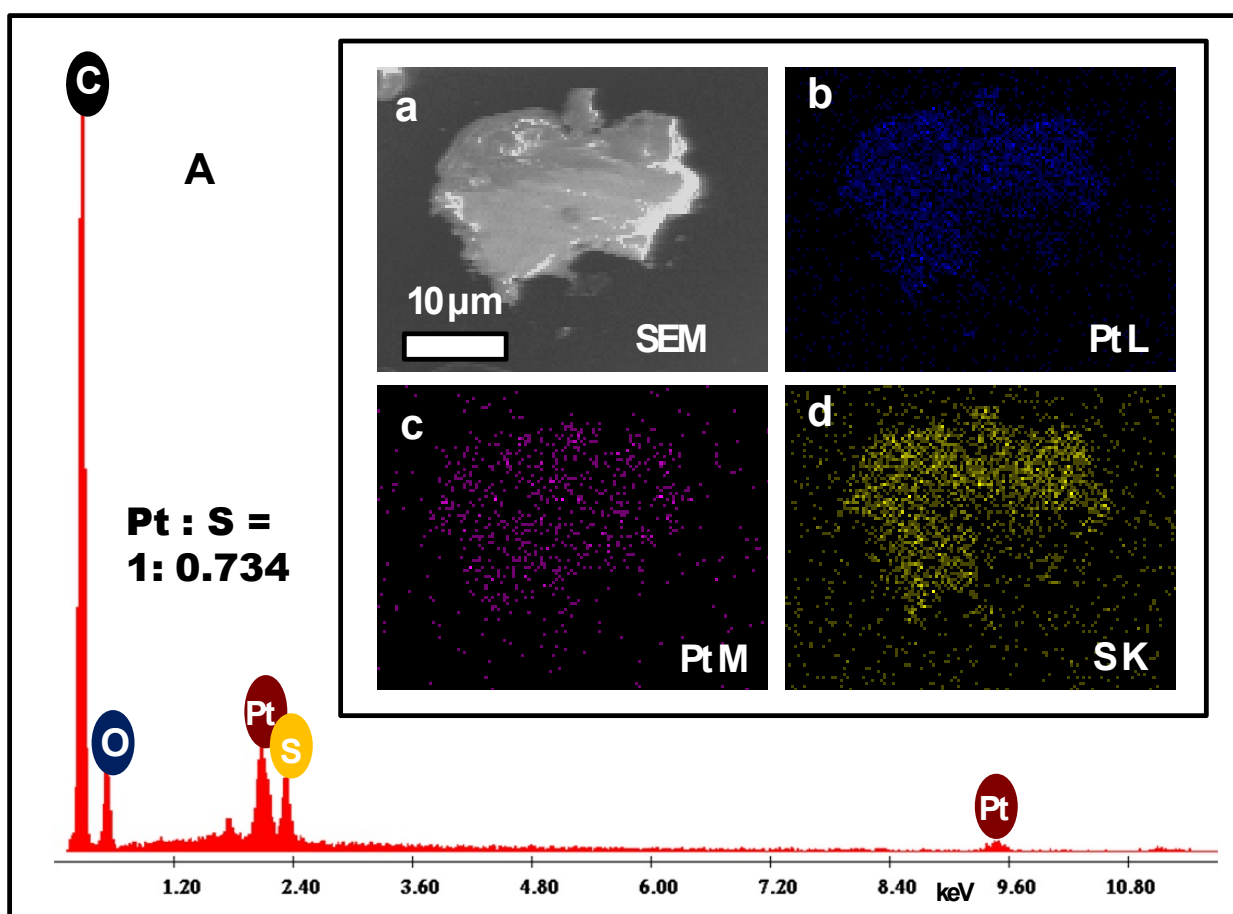


Fig. S10. A: SEM/EDAX spectrum of purified cluster showing all the expected elements. Pt:S ratio also supports the composition. Insets are the SEM image (a) and elemental maps of Pt L (b), Pt M (c) and S K (d).

Supporting Information 11

FT IR spectra of the thiol and cluster

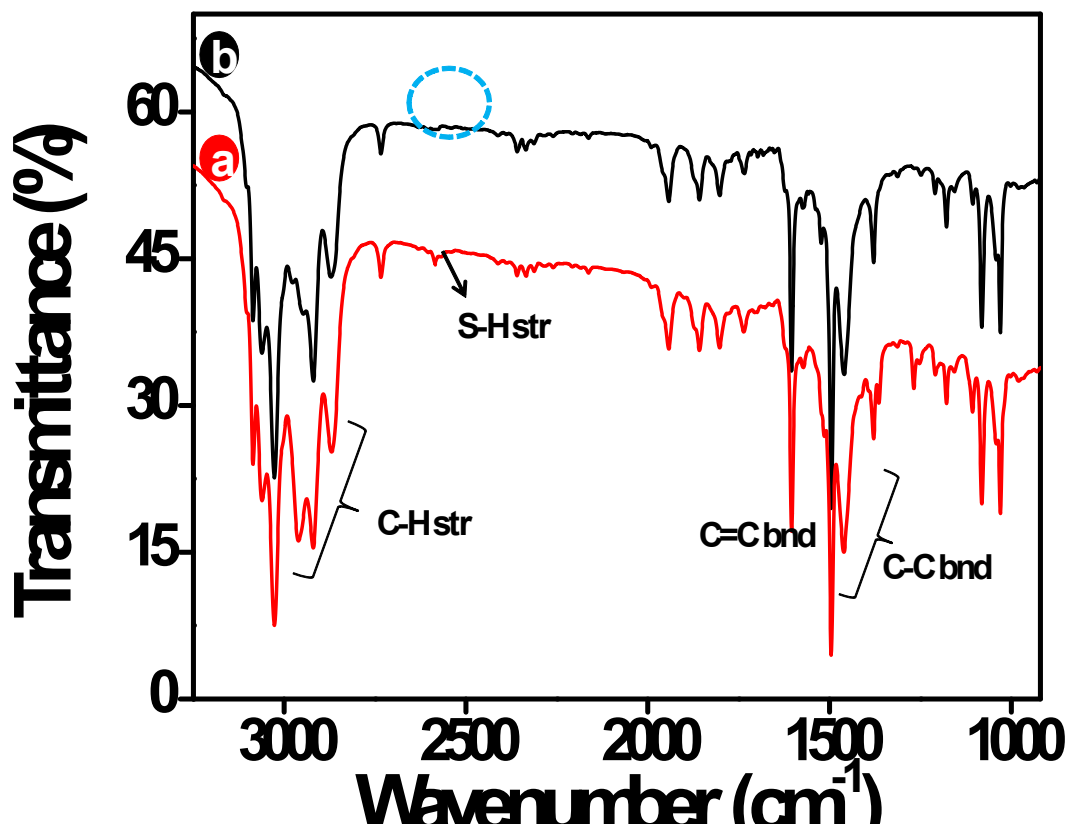


Fig. S11. The IR spectra of pure BBSH (a) and Pt₁₁(BBS)₈ cluster (b). The S-H stretching frequency at 2580 cm⁻¹ is absent in cluster which confirms the binding of thiol to the metal.

Supporting Information 12

XPS survey spectrum of the Pt₁₁(BBS)₈ cluster

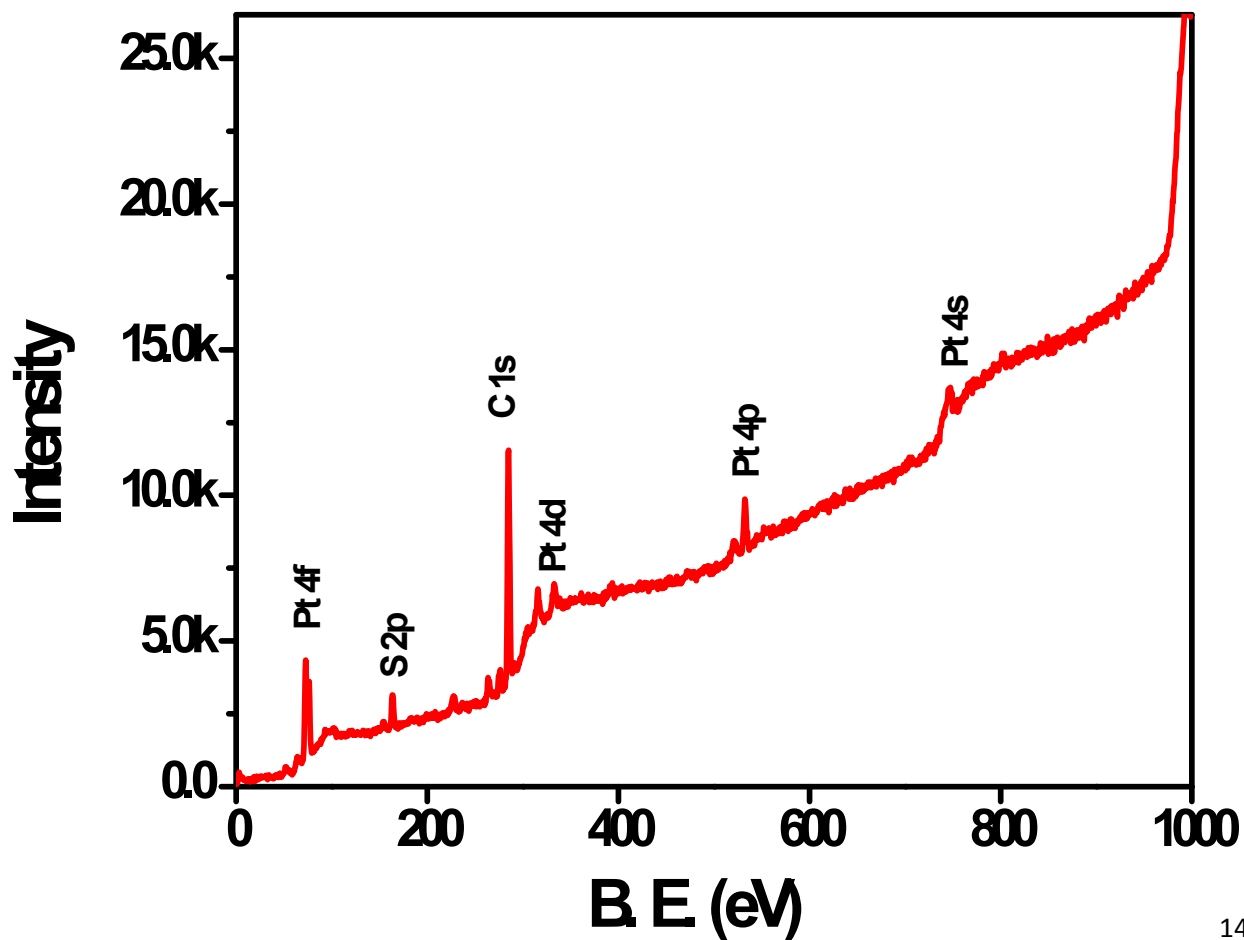


Fig. S12. XPS survey spectrum of the $\text{Pt}_{11}(\text{BBS})_8$ cluster. All the peaks are marked.

Supporting Information 13

Extended XPS spectra in the C 1s and S 2p regions

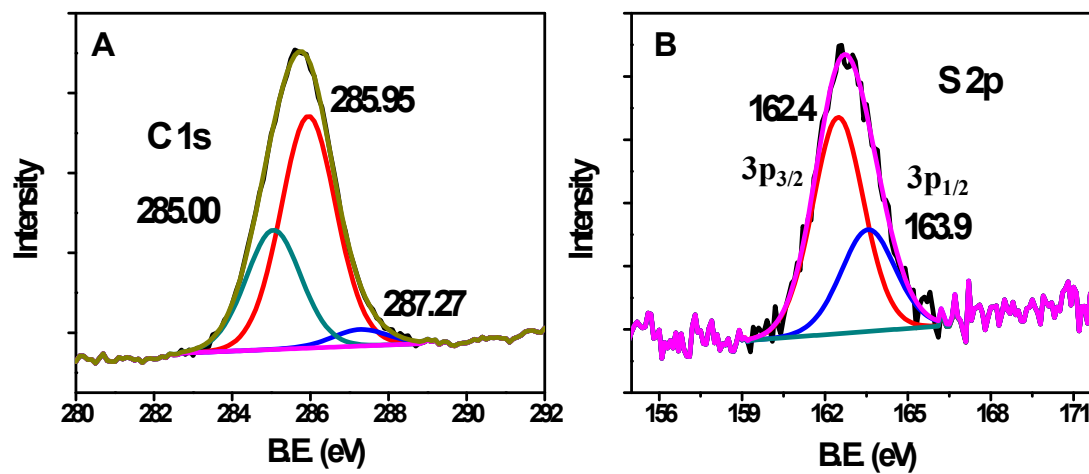


Fig. S13. Extended XPS spectra for C 1s (A), and S 2p (B) of the purified sample. Each spectrum was fitted with components.

Supporting Information 14

XRD of Pt₁₁(BBS)₈ cluster

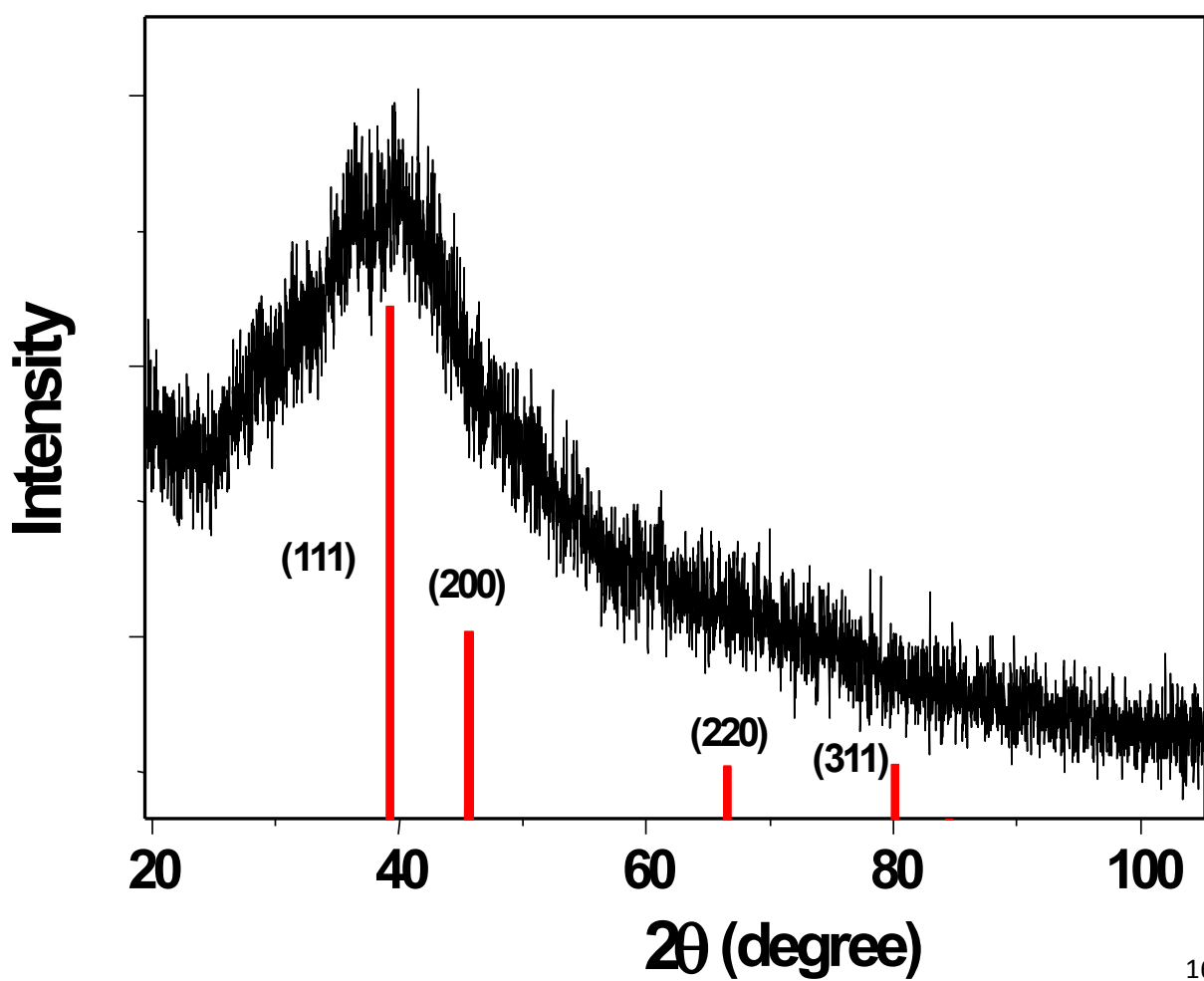


Fig. S14. X-ray diffraction patterns of as-synthesized Pt₁₁(BBS)₈ cluster. Positions of metallic platinum are shown for comparison.

Supporting Information 15

¹⁹⁵Pt NMR of K₂PtCl₆ standard

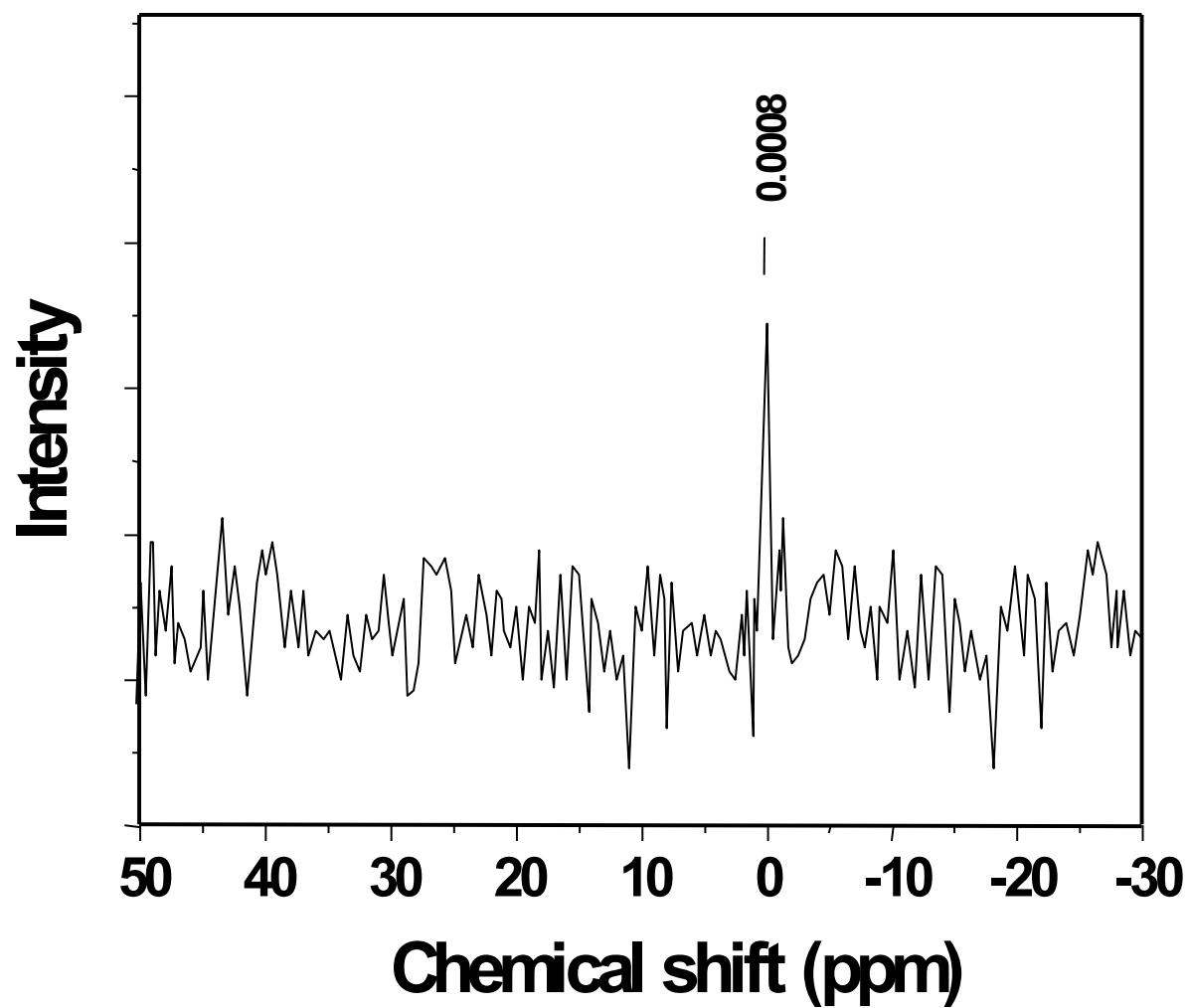


Fig. S15. ^{195}Pt NMR of K_2PtCl_6 standard (in D_2O).

Supporting Information 16

Time dependent UV/Vis and solvent compatibility

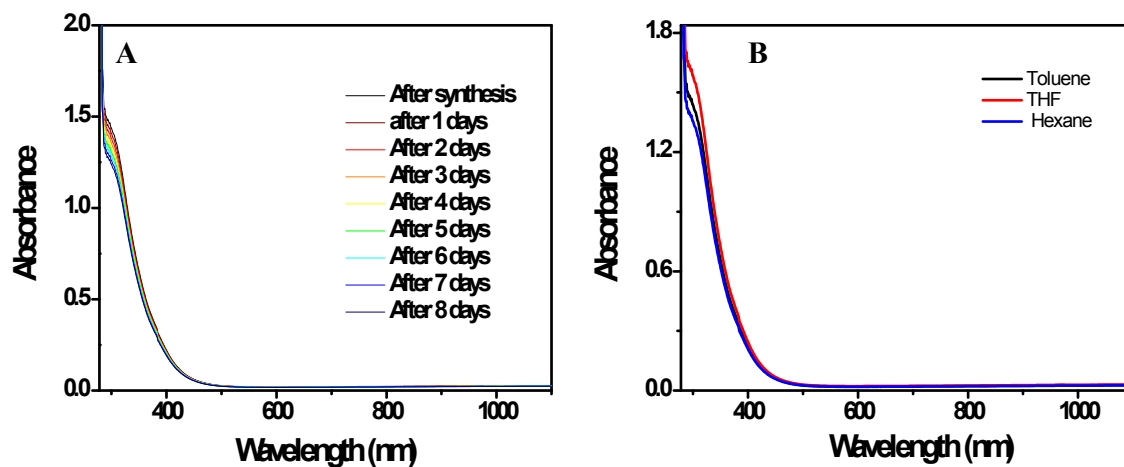


Fig. S16. Time dependent UV/Vis spectra of Pt₁₁ cluster (A) and UV/Vis spectra of the cluster extracted in different solvents (B).

1. Mohanty. J. S, Xavier P. L, Chaudhari K, Bootharaju M. S, Goswami N, Pal S. K and Pradeep T, *Nanoscale*, **2012**, *4*, 4255.